AJEMA GLOBAL RESEARCH NETWORK

AMERICAN Journal of Engineering, Mechanics and Architecture
Volume 02, Issue 06, 2024 ISSN (E): 2993-2637

RESEARCH OF FIRE RETARDANT PROPERTIES OF NEW COATINGS, PHOSPHATED ETHANOLAMINE BORATE ACIDS

Kodirov N.U, Beknazarov Kh.S
Doctor of Technical Sciences, Professor, Angreen University. Tashkent.

Ibragimov B.T.
Academy of the Ministry of Emergency Situations

Abstract. In this work we studied the synthesis of phosphonate triethanolamine borate (PTEAB-1). Take 10.8 g of triethanolamine borate substance (0.6 mmol) and dissolve in 50 ml of distilled water, place in a 100 ml two-neck round-bottom flask, select phosphorous acid (4.92 g or 0.6 mmol) and dissolve in 2-3 ml of distilled water to prepare the solution. In the next step, a 37% HCHO solution (0.726 g or 8.94 mmol) was slowly added to this heated solution under an inert nitrogen atmosphere and the process was carried out at 115 °C for 24 hours. Fourier transform infrared (FTIR) spectra were recorded on an IRAffinity-1S FTIR spectrometer (Shimadzu, Japan).
Keywords: Ethanolamine, borate acids, fire retardant, phosphorous acid.

Introduction The use of intumescent fire-retardant coatings is one of the most promising methods for reducing the fire hazard of wood and wood products. Typically, intumescent coatings consist of an appropriate binder and a combination of an acid source, a gas source, and a carbon source that can form a cell expansion layer that acts as a physical barrier against heat and mass transfer when exposed to flame and high temperature [1]. Currently, transparent intumescent fire retardant coatings are considered a highly effective material for protecting ancient buildings, cultural relics and high-quality wooden furniture from fire while maintaining their original appearance [2]. However, the production of transparent fire retardant coatings faces a huge challenge since both super-optical transparency and fire resistance are usually competitive properties [3]. In particular, traditional flame retardants to realize fire retardancy usually cause severe light scattering phenomenon due to the different refractive indices of the polymer matrix and flame retardants, resulting in loss of transparency [4]. The creation of transparent fire-retardant coatings based on a reactive fire retardant and an active polymer is a promising method for achieving a balance of fire resistance and optical transparency of coatings [5].

In this work, phosphatalated boric acid ethanolamine was synthesized and thoroughly characterized using FTIR and 1H NMR spectra.

Experimental part

Synthesis of phosphonated triethanolamine borate (PTEAB-1). Take 10.8 g of triethanolamine borate substance (0.6 mmol) and dissolve in 50 ml of distilled water, place in a 100 ml two-neck round-bottom flask, select phosphorous acid (4.92 g or 0.6 mmol) and dissolve in 2-3 ml of distilled water to prepare the solution. Next, a 37% hydrochloric acid solution (5.65 g or 35.8 mmol) is slowly added dropwise to the solution. In this case, the reaction is carried out by slowly heating to a temperature of 65 ° C in an oil bath under an inert nitrogen atmosphere.

In the next step, a 37% HCHO solution (0.726 g or 8.94 mmol) was slowly added to this heated solution under an inert nitrogen atmosphere and the process was carried out at 115 °C for 24 hours. After completion of the process, the resulting mixture is first slowly cooled to room temperature, and to neutralize the mixture, a 20% sodium alkali solution is added until the pH of the medium becomes ~6-7. The resulting mixture is evaporated to form a dry mass and sent to experimental processes. The acid number was 392.7.

The reaction mechanism for the synthesis of FTEAB-1 is shown in Scheme 1 and is described as follows.

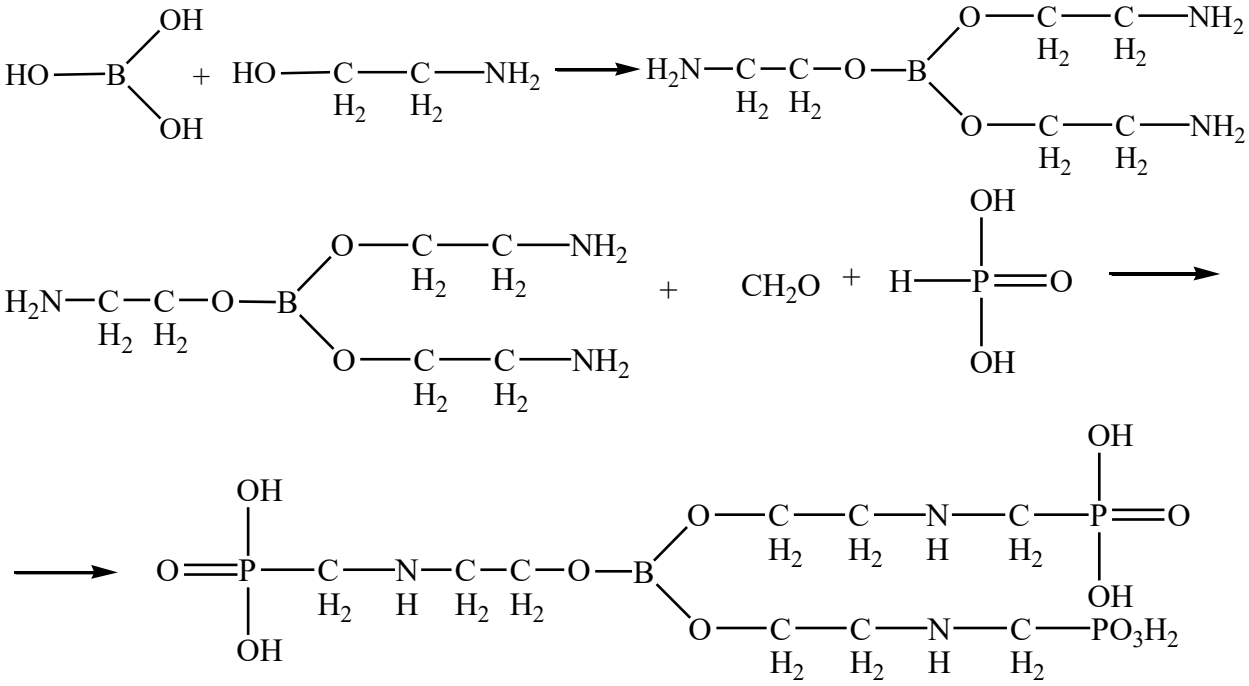

Scheme 1. Synthesis reaction scheme.

Preparation of amino-transparent fire-retardant coatings. Amino-transparent fire retardant coatings were prepared by mixing 100 g FTEAB-1 (60 wt%) and 120 g GMM (58–62 wt % in hexamethylolmelamine), where FTEAB-1 and GMM act as a hardener and fire retardant in the coatings. After 45 minutes of exposure, the resulting coatings were applied to plywood boards (100 mm × 100 mm × 4 mm, 150 mm × 150 mm × 4 mm and 600 mm × 90 mm × 4 mm) with a wet density of 500 g/m^2, and the coatings were cured to a film thickness of 0.4 ± 0.02 mm. The coating was applied to plywood boards with dimensions of 300×150×4 mm with a wet density of 250 g/m2, dry film thickness was 0.2±0.02 mm.

Fourier transform infrared (FTIR) spectra were recorded on an IRAffinity-1S FTIR spectrometer (Shimadzu, Japan).

^{1}H nuclear magnetic resonance (^{1}H NMR) spectra of FTEAB-1 were recorded on a Bruker Ascend 400 MHz NMR spectrometer (Bruker, Vällanden, Switzerland) using D2O as solvent.

Thermogravimetric (TG) analysis was performed on a Q60 instrument (TA Instruments, Linden, UT, USA). A sample weighing approximately 2 mg was placed on an alumina tray and then heated from 25°C to 800°C at a heating rate of 10°C/min under a nitrogen flow of 40 ml/min. Cabinet testing was carried out to record the weight loss, char index and swelling coefficient of coatings

applied to wood substrates in accordance with ASTM D1360-2011 using a Fire Retardant Paint Tester Type XSF-1 (Small Room Mode) with a sample size of 300 mm × 150 mm ± 4 mm.
Tunnel testing was conducted to measure the flame spread rate (FSR) of the specimens in accordance with ASTM D3806-2011 using a 2-ft SDF-2 type tunnel flame apparatus with a specimen size of 600 mm ± 90 mm ± 4 mm.
Thermal insulation testing was carried out to record the backside temperature of the samples using a cone calorimeter (Fire Testing Technology, East Grinstead, UK) at an external heat flux of 50 kW/m2. During the tests, a sample covered with transparent coatings was horizontally exposed to a thermal radiator with a distance between the coating and the bottom of the radiator of 25 ± 1 mm.
Cone calorimeter testing was used to measure the heat release rate and total heat release of the coatings using a cone calorimeter (Fire Testing Technology, East Grinstead, UK) in accordance with ISO5660-2002. Each sample measuring 100×100×4 mm was horizontally exposed to a heat sink under an external heat flux of 50 kW/m2.
Scanning electron microscope (SEM) images of coal residues were observed on a MIRA 3 LMU scanning electron microscope (Tescan, Brno, Czech Republic) at an accelerating voltage of 20 kV. Elemental analysis of the coal residues was measured using energy dispersive X-ray spectroscopy (EDS) cards on an X-Max20 X-ray probe (Oxford Instruments, Aylesbury, UK).
Accelerated aging testing was carried out in a UV weathering chamber (Dongguan HaoRan Testing Instrument Co. Ltd, Guangdong, China) in accordance with ASTM G154-2006. The samples were subjected to cycles of UV irradiation and condensation at regular intervals. Each cycle included 8 hours of UV irradiation at a black bulb temperature of 60±3°C and 4 hours of condensation at a black bulb temperature of 50±3°C. The radiation wavelength was 340 nm, and the UV radiation intensity was 0.76 W/(m^2 nm). Samples were removed from the aging oven after 2, 6 and 11 cycles for various measurements and characterization.

Results and Discussion

The FTIR spectra of FTEAB-1 are shown in Figure 1. In the spectra of FTEAB, the broad absorption peaks at 3400 and 1647 cm^{-1} are attributed to –OH groups. The characteristic peaks at 2872, 1456, 1336, 1016 and 673 cm^{-1} are attributed to the stretching vibrations of –CH_2– groups, B–O groups, B–O–C groups, C–O–C groups and BO3 groups. respectively. Notably, a new absorption peak of B–O–C groups appears at 1396 cm^{-1}, confirming the successful synthesis of FTEAB-1 products.

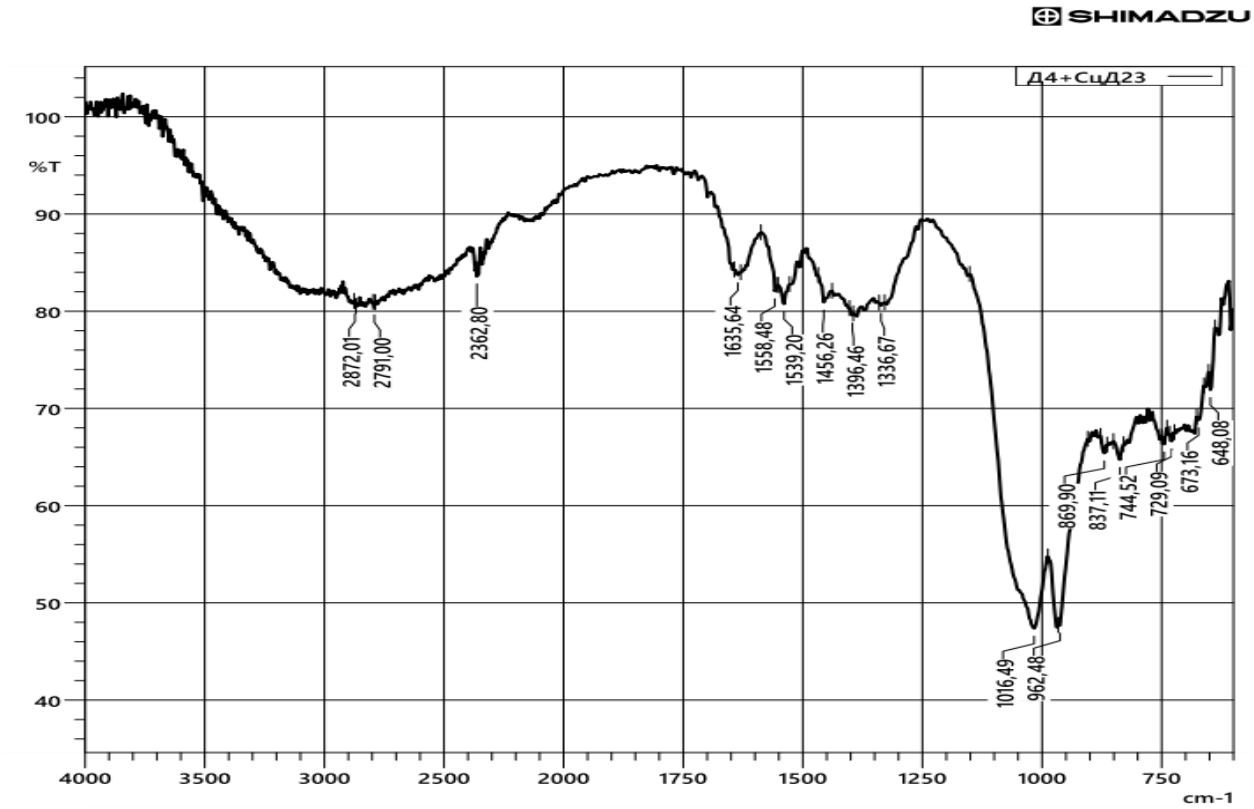

Fig.1. IR spectrum of FTEAB-1.

The ^{1}H NMR spectra of FTEAB-1 are presented in Figure 2. In the spectrum of FTEAB-1 there are two main signals located at 6.133 ppm. and 2.596 ppm, refer to the methylene protons in the cyclic structure P–O–CH^{2}– (indicated by the number 4) and the methylene protons in the exocyclic structure P–O–CH2– (indicated by the numbers 2, 3), respectively. Moreover, 0.09 ppm assigned to the methylene protons in ethanolamine. In the spectra of FTEAB, the peaks of methylene protons in the exocyclic structure of P–O–CH$_2$– (labeled 3) have a higher frequency than the peaks of EA, which is attributed to the protons in the P–OH groups substituted by the high electronegativity of FTEAB-1. In addition, a new peak at 0.28–0.29 ppm. corresponds to the methylene protons in the EA chain (indicated by the number 2). All the above results confirm that FTEAB-1 were successfully synthesized as shown in Scheme 2.

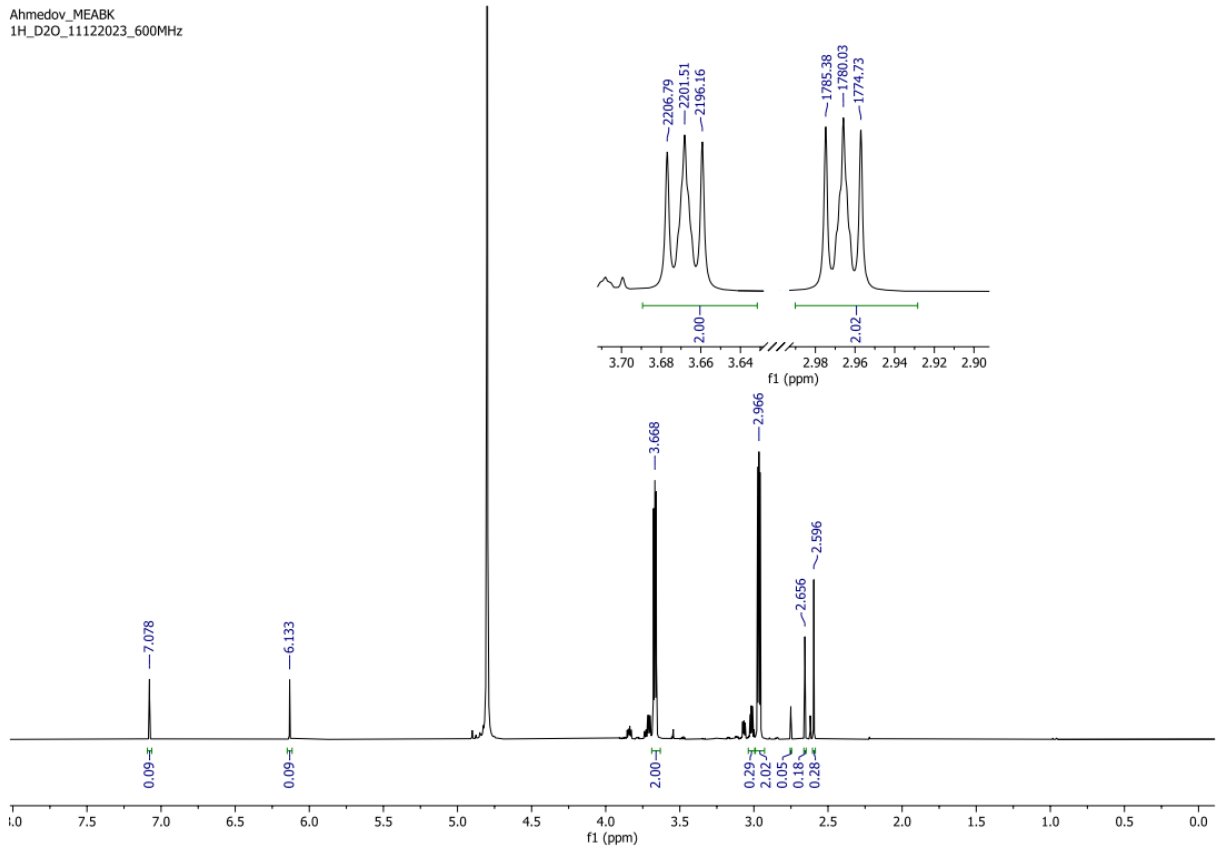

Rice. 2. ^{1}H NMR spectrum of FTEAB.

The TG and DTG curves of FTEAB coatings under nitrogen atmosphere are presented in Figure 3. The corresponding thermal parameters including the decomposition onset temperature at 5% mass loss (Ton), temperature at the maximum mass loss rate (Tmax), peak mass loss rate (PMLR) and residue at 700 oC are given in table. 1. In a nitrogen atmosphere, coatings exhibit four stages of decomposition, respectively, at 60–200 ºC, 200–300 ºC, 300–550 ºC. C and 550–700 ºC, where the third stage predominates. The first stage at 60–200 °C is associated with the release of small molecules of amino resin and phosphate esters. The second stage at 200–300 °C is associated with the cleavage of C–O–C groups in the pentaerythritol phosphate chain and the PEG chain, and FTEAB-1 coatings show higher weight loss and PMLR value due to the pyrolysis of FTEAB-1. The third stage at 300–550 °C is associated with the decomposition of amino resin and phosphoric acid esters; phosphoric acid derivatives and the ethanolamine ester chain decomposed from phosphoric acid esters interact with triazine derivatives and inert gases decomposing from amino resin to form multicellular coal. The fourth stage at 550–700°C is associated with the decomposition of unstable structures including C–C bonds or ether bonds in multicellular coal. The residue yield at 700 °C first increases and then decreases with the addition of FTEAB-1, indicating that the addition of EA enhances the charring ability of the coatings. In particular, FTEAB-1 gives the resulting coatings the highest residual weight among the samples, 36.3% at 700°C.

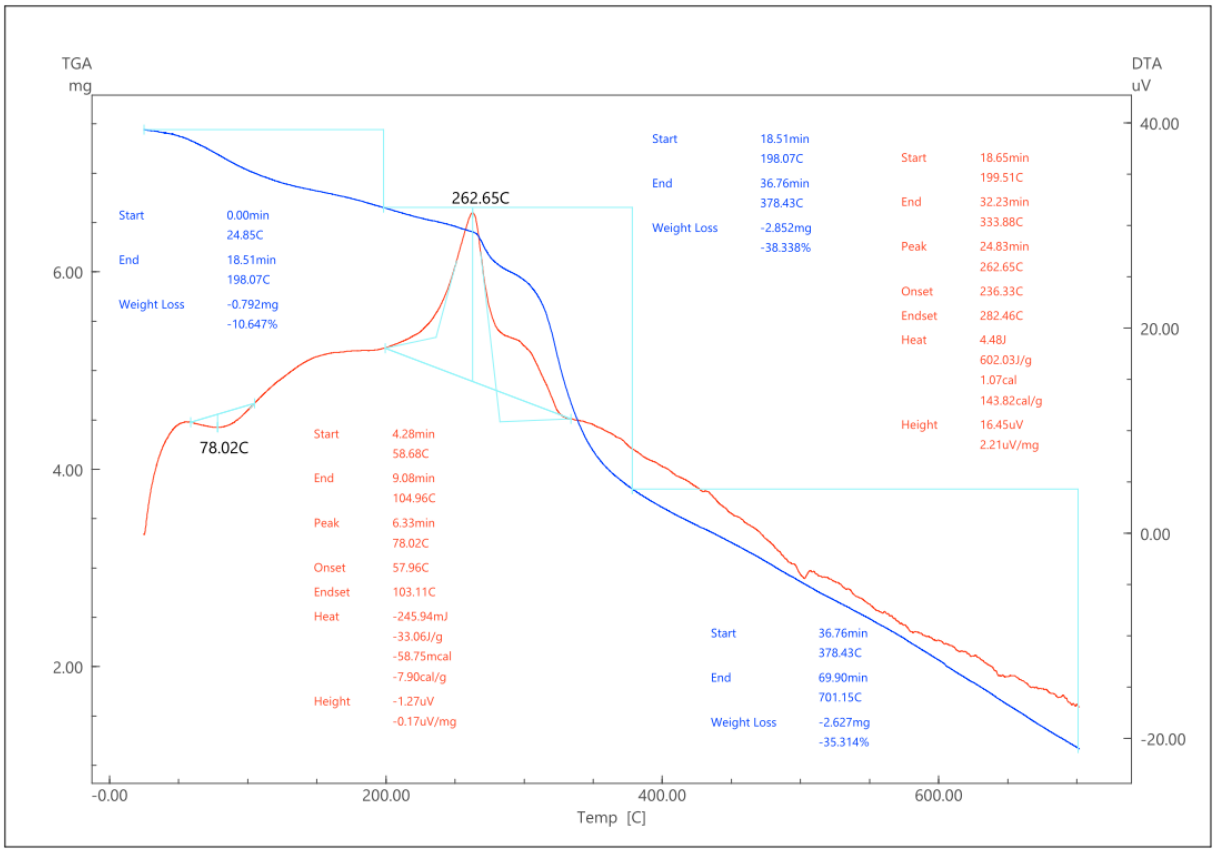

Fig.3. TG and DTG analysis FTEAB-1.

Table-1.

Thermal parameters of FTEAB-1 coatings in a nitrogen atmosphere.

Sample	Ton/°C	T_{max}/°C	MYYP/(%/min)	Residue at 700 oC/%
ФТЭАБ-1	262,65	375,4 c	3.2	27.8

From Table 1 it can be seen that the temperature of the onset of decomposition (Ton) of the coatings gradually increases the thermal stability of FTEAB-1, which means an increase in the thermal stability of the coatings. In addition, the formation of char in the coatings first increases and then decreases in the samples, and then inhibits the formation of char in the coatings. Thus, the introduction of a fire-retardant coating helps to increase both the thermal stability and charring of coatings.

The fire resistance analysis was carried out according to the above method. The temperature curves of the back side of the coatings obtained from the thermal insulation test are presented in Figure 4. As can be seen from Figure 4, the back side temperature of the uncoated plywood board increases rapidly and reaches a value above 260°C in 180 minutes. Application of coatings significantly reduces the temperature of the back side of the plywood board, which indicates an increase in thermal insulation properties. Equilibrium rear side temperature at 900 min. is 265.7 oC. It can be seen that the equilibrium temperature of the reverse side at 900 minutes of coatings first decreases and then increases with increasing concentration of FTEAB-1. These results

indicate that the addition of FTEAB-1 has a positive effect on increasing the thermal insulation properties of coatings, and the resulting coatings counteract the fire retardant effect. In particular, it gives coatings better thermal insulation properties.

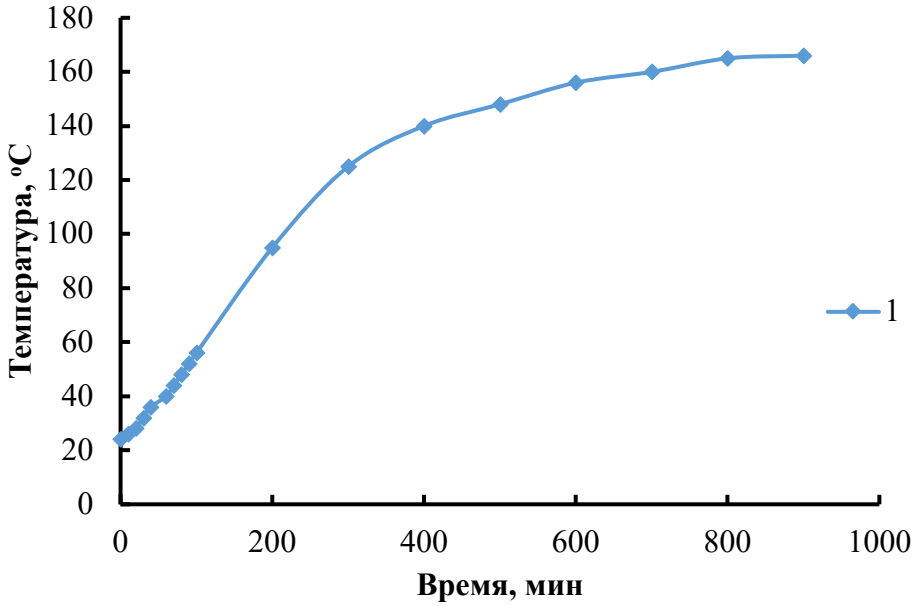

Rice. 4. Temperature curves of the back side of a wood substrate coated with a transparent fire retardant coating.

Conclusion.

The synthesized FTEAB-1 coating was successfully grafted onto the phosphorous acid structure, and the chemical structure of FTEAB was thoroughly characterized by FTIR and 1H NMR spectra. The resulting FTEAB-1 was mixed with amino resin to obtain amino-transparent fire-retardant coatings, and the effect of FTEAB-1 on the mechanical properties and fire resistance of coatings was assessed by various analytical methods. TG analysis shows that the presence of FTEAB-1 contributes to an increase in the residual mass of the coatings. In particular, FEAB-1 exhibits the highest residual mass of 36.3% at 700 °C. Fire retardant and cone calorimetry tests show that the addition of FTEAB-1 enhances the fire retardant effect of coatings. In particular, FTEAB-1 has the best flame retardant effect, showing a 28.5% reduction in peak heat release rate and a 57.6% reduction in flame propagation rate.

References

1. Alongi, J.; Han, Z.; Bourbigot, S. Intumescence: Tradition versus novelty. A comprehensive review. Prog. Polym. Sci. **2015**, 51, 28–73. [CrossRef]
2. Shree, R.; Naik, R.B.; Gunasekaran, G. Effect of three structurally different epoxy resins on fire resistance, optical transparency, and physicomechanical properties of intumescent fire-retardant transparent coatings. J. Coat. Technol. Res. **2021**, 18, 535–547. [CrossRef]
3. Loste, J.; Lopez-Cuesta, J.-M.; Billon, L.; Garay, H.; Save, M. Transparent polymer nanocomposites: An overview on their synthesis and advanced properties. Prog. Polym. Sci. **2019**, 89, 133–158. [CrossRef]

4. Xu, Z.; Xie, X.; Yan, L.; Feng, Y. Fabrication of organophosphate-grafted kaolinite and its effect on the fire-resistant and anti-ageing properties of amino transparent fire-retardant coatings. Polym. Degrad. Stab. **2021**, 188, 109589. [CrossRef]

5. Xu, Z.; Deng, N.; Yan, L. Flame retardancy and smoke suppression properties of transparent intumescent fire-retardant coatings reinforced with layered double hydroxides. J. Coat. Technol. Res. **2020**, 17, 157–169. [CrossRef].

6. Nomozov A K, Beknazarov Kh S, Khodjamkulov S Z, Misirov Z Kh. Salsola Oppositifolia acid extract as a green corrosion inhibitor for carbon steel. Indian J Chem *Tech*. 2023; 30(6)**:** 872-877. https://doi.org/10.56042/ijct.v30i6.6553.

7. Muratov B.A, Turaev Kh. Kh, Umbarov I.A, Kasimov Sh.A, Nomozov A.K, "Studying of Complexes of Zn(II) and Co(II) with Acyclovir (2-amino-9-((2-hydroxyethoxy)methyl)-1,9-dihydro-6H-purine-6-OH),"*Int. J of Eng. Trends and Tech.* 2024; 72(1): 202-208. https://doi.org/10.14445/22315381/IJETT-V72I1P120.

8. Shaymardanova M A, Mirzakulov Kh Ch, Melikulova G, Khodjamkulov S Z, Nomozov A K, Shaymardanova Kh.S. Study of process of obtaining monopotassium phosphate based on monosodium phosphate and potassium chloride. Chemical Problems. 2023; 3 (21): 279-293. https://doi.org/10.32737/2221-8688-2023-3-279-293.